

Scaled Relative Graphs for Nonmonotone Operators with Applications in Circuit Theory

Jan Quan

Brecht Evens

Rodolphe Sepulchre

Panagiotis Patrinos

Abstract—The scaled relative graph (SRG) is a powerful graphical tool for analyzing the properties of operators, by mapping their graph onto the complex plane. In this work, we study the SRG of two classes of nonmonotone operators, namely the general class of semimonotone operators and a class of angle-bounded operators. In particular, we provide an analytical description of the SRG of these classes and show that membership of an operator to these classes can be verified through geometric containment of its SRG. To illustrate the importance of these results, we provide several examples in the context of electrical circuits. Most notably, we show that the Ebers–Moll transistor belongs to the class of angle-bounded operators and use this result to compute the response of a common-emitter amplifier using Chambolle–Pock, despite the underlying nonsmoothness and multi-valuedness, leveraging recent convergence results for this algorithm in the nonmonotone setting.

I. INTRODUCTION

Recently, the scaled relative graph (SRG) has emerged as a powerful tool for analyzing individual operators and their interconnections. Originally introduced in [1], the SRG can be interpreted as a generalization of the classical Nyquist diagram to arbitrary nonlinear operators. By mapping an operator’s graph onto the complex plane, the SRG provides insights into its incremental gain and phase properties, with interconnections represented as graphical manipulations of SRGs. For instance, this approach unifies and extends classical results like the Nyquist criterion and the incremental passivity theorem [2], and can be used as a formal framework for constructing geometric proofs of convergence for contractive and nonexpansive fixed-point iterations, with similar 2D visualizations appearing earlier in [3], [4]. Central to this approach is the concept of SRG-full operator classes, where membership of an operator to such classes directly corresponds to the geometric containment of its SRG. SRG-full classes include many common operator classes defined through inequalities, such as (hypo)monotone, co(hypo)monotone, Lipschitz, and averaged operators [1].

In many applications, operators belonging to these classes emerge quite naturally. For instance, in circuit theory many commonly used circuit elements such as linear time-invariant

resistors, capacitors, inductors, transformers and gyrators are known to be maximally monotone [5], [6]. Based on this observation, [5] demonstrated that the behavior of a monotone circuit can be modeled as the zero of a monotone + skew inclusion problem, where the monotone component represents the device equations and the skew component arises from the circuit topology by Tellegen’s theorem [7]. This type of inclusion problem can be solved in an efficient manner using the Chambolle–Pock iteration [8]. Compared to traditional methods based on ordinary differential equations, this splitting method offers greater scalability, robustness to parameter variations, and is able to deal with nonsmooth and multi-valued elements.

However, besides these monotone circuit elements, there are also several commonly used circuit elements which exhibit complicated *nonmonotone* behavior, not properly captured by any previously mentioned SRG-full operator class. Notable examples include the tunnel diode, transistor devices, nonlinear capacitors/inductors and memristive elements. For instance, using the SRG it was observed in [6] that the potassium conductance in the Hodgkin–Huxley membrane model [9] is hypomonotone, although it also exhibits stronger properties which this class does not adequately capture.

In this work, we will address this issue by considering two classes of nonmonotone operators which are more suitable for accurately capturing the nonmonotone behavior of these circuit elements, namely *semimonotone operators* and *angle-bounded operators*. The class of semimonotone operators was first introduced in [10] and can be used to derive sufficient conditions for several splitting methods in the nonmonotone setting, including Chambolle–Pock [11]. This class was recently studied in [12] for networks consisting only of memristors. The class of angle-bounded operators is inspired by the singular angle introduced in [13]. The singular angle is the phase counterpart of the L_2 -gain, capturing the amount of rotation induced by a system.

Our main contributions are as follows:

- (i) We derive an analytical expression for the SRGs of semimonotone and angle-bounded operators, and show that both are SRG-full. Additionally, we establish a connection between these two classes of operators through the SRG.
- (ii) We show that Ebers–Moll transistors are angle-bounded under standard assumptions, and as a result also semimonotone.
- (iii) We consider common-emitter amplifiers involving transistors and tunnel diodes. Despite the nonsmoothness, nonmonotonicity, and potential multi-valuedness

This work was supported by the Research Foundation Flanders (FWO) PhD grant 1183822N and research projects G081222N, G033822N, and G0A0920N; Research Council KUL grant C14/24/103; and the European Research Council under the European Union’s Horizon 2020 research and innovation program / ERC Advanced Grant: SpikyControl (no. 7101054323).

KU Leuven, Department of Electrical Engineering ESAT-STADIUS – Kasteelpark Arenberg 10, box 2446, 3001 Leuven, Belgium
{jan.quan,brecht.evens,rodolphe.sepulchre,panos.patrinos}@kuleuven.be

of these elements, we show that their response can be computed efficiently using the Chambolle–Pock algorithm, building on recent convergence results for semimonotone operators from [11]. Due to the aforementioned difficulties, standard Newton methods are not applicable in this setting, highlighting the merits of our results.

A. Notation

We denote the set of complex and extended-complex numbers by \mathbb{C} and $\overline{\mathbb{C}} := \mathbb{C} \cup \{\infty\}$ respectively. The graph of a set-valued mapping $A : \mathcal{H} \rightrightarrows \mathcal{H}$ on a Hilbert space \mathcal{H} is defined as $\mathbf{gph} A := \{(x, y) \in \mathcal{H} \times \mathcal{H} \mid y \in A(x)\}$. We denote the identity operator on a suitable space by id . For scalars and sets, Minkowski-type operations are to be understood, i.e., $A + B := \{a + b \mid a \in A, b \in B\}$ and $\alpha A := \{\alpha a \mid a \in A\}$. An operator class \mathcal{A} is a set of operators on Hilbert spaces. The open disk with center $c \in \mathbb{C}$ and radius $r > 0$ is defined as $D(c, r) := \{z \in \mathbb{C} \mid \|z - c\| < r\}$.

II. SCALED RELATIVE GRAPHS

First, we introduce the concept of scaled relative graphs, which map the incremental properties of an operator $A : \mathcal{H} \rightrightarrows \mathcal{H}$ to a subset of the extended complex plane $\overline{\mathbb{C}}$.

Consider a pair $(x, u), (y, v) \in \mathbf{gph} A$ and define the corresponding complex conjugate pair

$$z_{\pm}(x - y, u - v) := \frac{\|u - v\|}{\|x - y\|} \exp(\pm i \angle(x - y, u - v)),$$

where the angle $\angle(x - y, u - v)$ is defined as

$$\begin{cases} \arccos\left(\frac{\langle x - y, u - v \rangle}{\|x - y\| \|u - v\|}\right) & \text{if } x \neq y \text{ and } u \neq v, \\ 0 & \text{otherwise.} \end{cases}$$

By considering all different pairs, the scaled relative graph of operators and operator classes can be constructed as follows.

Definition II.1. *The SRG of an operator A is defined as*

$$G(A) := \left\{ z_{\pm}(x - y, u - v) \mid u \in A(x), v \in A(y), x \neq y \right\} \left(\cup \{\infty\} \text{ if } A \text{ is multi-valued} \right)$$

and the SRG of an operator class \mathcal{A} is defined as

$$G(\mathcal{A}) := \bigcup_{A \in \mathcal{A}} G(A).$$

By construction, the SRG thus provides a visualization of the incremental gain and phase of all input-output pairs of an operator (or an operator class). However, the real power of the SRG shines through for SRG-full classes.

Definition II.2. *An operator class \mathcal{A} is SRG-full if*

$$A \in \mathcal{A} \Leftrightarrow G(A) \subseteq G(\mathcal{A}).$$

In essence, a class is SRG-full if membership of an operator to that class is equivalent to the geometric containment of its SRG. In this paper, we will focus on SRG-full classes

defined by a nonnegatively homogeneous function h , i.e., a function for which $h(\eta a, \eta b, \eta c) = \eta h(a, b, c)$ for all $\eta \geq 0$.

Proposition II.3. ([1, Thm. 2]) *An operator class \mathcal{A} is SRG-full if there is a nonnegatively homogeneous function $h : \mathbb{R}^3 \rightarrow \mathbb{R}$ such that*

$$A \in \mathcal{A} \Leftrightarrow h(\|u - v\|^2, \|x - y\|^2, \langle x - y, u - v \rangle) \leq 0, \quad \forall (x, u), (y, v) \in \mathbf{gph} A.$$

Notable examples of such operator classes include the classes of (hypo)monotone, co(hypo)monotone, Lipschitz, and averaged operators [1].

Before proceeding, we recall some important calculus rules for SRGs which will be used throughout the paper.

Proposition II.4. ([1, Thms. 4&5]) *Let \mathcal{A} be an operator class, and let $\alpha \in \mathbb{R} \setminus \{0\}$. Then, the following equations hold.*

- (i) $G(\alpha \mathcal{A}) = G(\mathcal{A} \alpha) = \alpha G(\mathcal{A})$
- (ii) $G(\text{id} + \mathcal{A}) = 1 + G(\mathcal{A})$
- (iii) $G(\mathcal{A}^{-1}) = (G(\mathcal{A}))^{-1} = \{\frac{1}{r} e^{i\varphi} \mid r e^{i\varphi} \in G(\mathcal{A})\}$

As an example of these calculus rules, consider the SRG of the class of monotone operators, given by

$$G(\mathcal{M}) = \{z \in \mathbb{C} \mid \text{Re } z \geq 0\} \cup \{\infty\}.$$

By Proposition II.4, it follows immediately that the SRGs of the class of μ -monotone operators $\mathcal{M}_{\mu} = \mu \text{id} + \mathcal{M}$ and ρ -comonotone operators $\mathcal{C}_{\rho} = \mathcal{M}_{\rho}^{-1}$ are given by

$$G(\mathcal{M}_{\mu}) = \{z \in \mathbb{C} \mid \text{Re } z \geq \mu\} \cup \{\infty\}, \quad (1)$$

$$G(\mathcal{C}_{\rho}) = \begin{cases} \overline{\mathbb{C}} \setminus D\left(\frac{1}{2\rho}, \frac{1}{2|\rho|}\right) & \text{if } \rho < 0, \\ \text{cl } D\left(\frac{1}{2\rho}, \frac{1}{2|\rho|}\right) & \text{if } \rho > 0, \end{cases} \quad (2)$$

where cl denotes the closure of a set. A visualization of these SRGs is provided in Figure 1.

III. SRGS OF NONMONOTONE OPERATORS

In this section, we examine the scaled relative graph of two recently introduced classes of nonmonotone operators, namely semimonotone and angle-bounded operators. We start by defining the semimonotone class, first introduced in [10, Def. 4.1].

Definition III.1. *Let $\mu, \rho \in \mathbb{R}$. A set-valued operator $A : \mathcal{H} \rightrightarrows \mathcal{H}$ is (μ, ρ) -semimonotone if*

$$\langle x - y, u - v \rangle \geq \mu \|x - y\|^2 + \rho \|u - v\|^2, \quad \forall (x, u), (y, v) \in \mathbf{gph} A.$$

It is maximally (μ, ρ) -semimonotone if its graph is not strictly contained in the graph of any other (μ, ρ) -semimonotone operator. The set of (μ, ρ) -semimonotone operators will be denoted by $\mathcal{S}_{\mu, \rho}$.

Since this class is defined through the nonnegatively homogeneous function $h : (a, b, c) \mapsto \rho a + \mu b - c$, it is SRG-full by Proposition II.3.

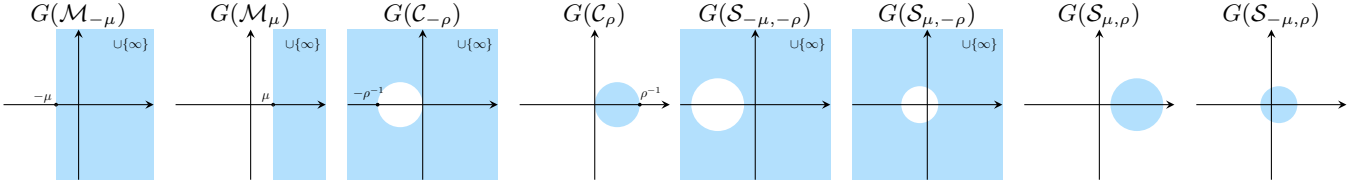


Fig. 1: Scaled relative graphs of several (hypo)monotone, co(hypo)monotone and semimonotone operators, where $\mu, \rho \in \mathbb{R}_{++}$. The center and diameter of the emerging circles in the SRGs depend on μ and ρ (see Proposition III.4). For the SRG of other operator classes, we refer to [1].

Proposition III.2. $\mathcal{S}_{\mu, \rho}$ is SRG-full for any $\mu, \rho \in \mathbb{R}$.

Note that this operator class generalizes many well-known operator classes in the literature, including monotone and comonotone operators ($\mathcal{S}_{0,0} = \mathcal{M}$, $\mathcal{S}_{\mu,0} = \mathcal{M}_{\mu}$ and $\mathcal{S}_{0,\rho} = \mathcal{C}_{\rho}$). Equivalences with other operator classes are detailed in [10, Rem. 4.2].

Now, we recall a calculus rule for the sum of a semimonotone operator with identity from [10, Prop. 4.8], which is then used alongside Proposition II.4 to obtain the analytical expression for the SRG of a semimonotone operator.

Proposition III.3. Let $A : \mathcal{H} \rightrightarrows \mathcal{H}$ be (maximally) (μ, ρ) -semimonotone and consider $B = A + \alpha \text{id}$ with $\alpha \in \mathbb{R}$. If $1 + 2\rho\alpha > 0$, then B is (maximally) $\left(\frac{\mu + \alpha(1 + \rho\alpha)}{1 + 2\rho\alpha}, \frac{\rho}{1 + 2\rho\alpha}\right)$ -semimonotone.

Proposition III.4. Let $\mu, \rho \in \mathbb{R} \setminus \{0\}$ such that $\mu\rho < \frac{1}{4}$. Let $c = \frac{1}{2\rho}$ and $r = \frac{\sqrt{1 - 4\mu\rho}}{2|\rho|}$. Then the SRG of the operator class of (μ, ρ) -semimonotone operators is given by

$$G(\mathcal{S}_{\mu, \rho}) = \begin{cases} \overline{\mathbb{C}} \setminus D(c, r) & \text{if } \rho < 0, \\ \text{cl } D(c, r) & \text{if } \rho > 0. \end{cases}$$

Proof. Let $\alpha = \frac{-1 + \sqrt{1 - 4\mu\rho}}{2\rho}$ and note that $1 + 2\rho\alpha > 0$. Consequently, it follows from Proposition III.3 that $\mathcal{S}_{\mu, \rho} + \alpha \text{id} = \mathcal{S}_{0, \beta} = \mathcal{C}_{\beta}$ where $\beta = \frac{\rho}{1 + 2\rho\alpha}$. The result then immediately follows from (2) and Propositions II.4(i), II.4(ii), using the fact that $\frac{1 + 2\rho\alpha}{2\rho} - \alpha = \frac{1}{2\rho}$ and $\frac{1 + 2\rho\alpha}{2|\rho|} = \frac{\sqrt{1 - 4\mu\rho}}{2|\rho|}$. \square

There are four qualitatively different SRGs for semimonotone operators, depending on the signs of μ and ρ . These are shown in Figure 1.

Remark III.5. If $\mu < 0$, $\rho < 0$ and $\mu\rho \geq \frac{1}{4}$, then all operators are (μ, ρ) -semimonotone. Similarly, if $\mu > 0$, $\rho > 0$ and $\mu\rho > \frac{1}{4}$, then there exist no operators that are (μ, ρ) -semimonotone [10, Prop. 4.3].

Having established the SRG of the class of semimonotone operators, we continue with a class of angle-bounded operators, defined as follows.

Definition III.6. Let $\theta \in [0, \pi]$. A set-valued operator $A : \mathcal{H} \rightrightarrows \mathcal{H}$ is θ -angle-bounded if

$$\angle(x - y, u - v) \leq \theta, \quad \forall (x, u), (y, v) \in \mathbf{gph} A,$$

or equivalently if

$$\langle x - y, u - v \rangle \geq \cos(\theta) \|x - y\| \|u - v\|. \quad (3)$$

The set of all θ -angle-bounded operators is denoted by \mathcal{B}_{θ} .

This notion is closely related to the singular angle defined in [13]. By construction, the SRG of the class of θ -angle-bounded operators is given by

$$G(\mathcal{B}_{\theta}) = \{r e^{i\tilde{\theta}} \mid r \in \mathbb{R}_+, \tilde{\theta} \in [-\theta, \theta]\} \cup \{\infty\}.$$

This SRG is visualized in Figure 2(a). Note that this operator class is also SRG-full as it is defined through the nonnegatively homogeneous function $h(a, b, c) = \cos(\theta) \sqrt{a} \sqrt{b} - c$. In what follows, we establish a connection between angle-bounded operators and semimonotone operators, which will be essential in the next section to show that the Ebers–Moll transistor is semimonotone under classical assumptions (see Corollary IV.5).

Proposition III.7. Let $\mu \in \mathbb{R}$, $\rho < 0$, $\alpha \geq 0$ and $\theta \in [\frac{\pi}{2}, \pi)$. If $1 - 4\mu\rho \leq (1 - 2\alpha\rho)^2 \sin^2(\theta)$, then $\mathcal{B}_{\theta} + \alpha \text{id} \subseteq \mathcal{S}_{\mu, \rho}$.

Proof. Let $A \in \mathcal{B}_{\theta} + \alpha \text{id}$. By Propositions III.2, III.4, it suffices to check that its SRG does not contain the disk with center $\frac{1}{2\rho} \in \mathbb{C}$ and radius $\frac{\sqrt{1 - 4\mu\rho}}{2|\rho|}$. Consider the construction in Figure 2(b). By the law of sines, the disk is not contained if

$$\frac{\sqrt{1 - 4\mu\rho}}{2|\rho|} \leq \sin(\theta) \left(\frac{1}{2|\rho|} + \alpha \right),$$

from which the claimed result follows immediately. \square

Note that there is a trade-off between μ and ρ , as there are many combinations for which Proposition III.7 is valid. This is visualized in Figure 2(c). When $\alpha > 0$, we can restrict our focus to the class of comonotone operators by setting $\mu = 0$ in Proposition III.7, resulting in the following corollary.

Corollary III.8. Let $\theta \in [\frac{\pi}{2}, \pi)$ and $\alpha > 0$. Then, $\mathcal{B}_{\theta} + \alpha \text{id} \subseteq \mathcal{C}_{\rho}$, where $\rho = \frac{1}{2\alpha} \left(1 - \frac{1}{\sin \theta}\right) < 0$.

IV. SEMIMONOTONICITY OF CIRCUIT ELEMENTS

This section examines the semimonotonicity of static nonlinearities and transistors, which will then be applied to common-emitter amplifier circuits in Section V.

A. One-dimensional static nonlinearities

Static nonlinearities are simple mathematical models which can be used to describe behaviors of certain circuit elements, such as nonlinear resistances and tunnel diodes. The following result, which can also be derived from [2, Prop. 9]

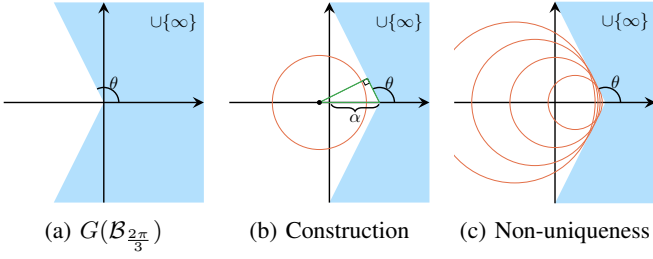


Fig. 2: The SRG of an angle-bounded operator and the construction to relate $\mathcal{B}_\theta + \alpha \text{id}$ to $\mathcal{S}_{\mu, \rho}$.

and [10, Prop. 4.14(iv)], shows that any one-dimensional static nonlinearity with a bounded slope is semimonotone. For clarity, we provide a self-contained proof here.

Proposition IV.1. *Let $T : \mathbb{R} \rightarrow \mathbb{R}$ be a one-dimensional single-valued operator and let $\ell > 0$ and $\sigma \in (-\ell, \ell]$. Then, the slope of T is bounded between σ and ℓ , i.e.,*

$$\sigma \leq \frac{T(x) - T(y)}{x - y} \leq \ell, \quad \forall x, y \in \mathbb{R}, x \neq y, \quad (4)$$

if and only if T is $(\frac{\sigma\ell}{\ell+\sigma}, \frac{1}{\ell+\sigma})$ -semimonotone.

Proof. Since $T : \mathbb{R} \rightarrow \mathbb{R}$ is one-dimensional and single-valued, it holds by Definition II.1 that

$$G(T) = \left\{ \frac{T(x) - T(y)}{x - y} \mid x, y \in \mathbb{R}, x \neq y \right\}.$$

Therefore, since the class of semimonotone operators is SRG-full, it follows from Propositions III.2, III.4 that T is $(\frac{\sigma\ell}{\ell+\sigma}, \frac{1}{\ell+\sigma})$ -semimonotone if and only if $G(T) \subseteq \text{cl} D(\frac{\ell+\sigma}{2}, \frac{\ell-\sigma}{2})$. Since this is equivalent to (4), the proof is completed. \square

Note that (4) is closely related to the notion of sector nonlinearities, which satisfy $\sigma \leq \frac{T(x)}{x} \leq \ell$ for all $x \in \mathbb{R}$. To highlight the importance of this result, consider its application to tunnel diodes: despite having a *negative resistance region*, these elements remain semimonotone as long as their slope is bounded, as illustrated below.

Example IV.2. Let $r_1, r_2, \bar{v} > 0$ with $r_1 < r_2$ and consider the piecewise linear tunnel diode

$$T_{\text{tunnel}} : \mathbb{R} \rightarrow \mathbb{R} : v \mapsto \begin{cases} r_1^{-1}(v + \bar{v}) + r_2^{-1}\bar{v}, & \text{if } v < -\bar{v}, \\ -r_2^{-1}v, & \text{if } |v| \leq \bar{v}, \\ r_1^{-1}(v - \bar{v}) - r_2^{-1}\bar{v}, & \text{if } v > \bar{v}. \end{cases}$$

By applying Proposition IV.1 with $\sigma = -r_2^{-1}$ and $\ell = r_1^{-1}$, it follows that T_{tunnel} is $(\frac{1}{r_1 - r_2}, \frac{r_1 r_2}{r_2 - r_1})$ -semimonotone.

B. Transistor

Let $R := \begin{pmatrix} 1 & -\alpha_R \\ -\alpha_F & 1 \end{pmatrix}$. An NPN transistor can then be represented using the Ebers–Moll model $T_{\text{NPN}} : \mathbb{R}^2 \rightrightarrows \mathbb{R}^2$, given by

$$T_{\text{NPN}} \left(\begin{matrix} v_1 \\ v_2 \end{matrix} \right) := \left\{ R \begin{pmatrix} u_1 \\ u_2 \end{pmatrix} \mid \begin{matrix} u_1 \in T_{\text{D}}(v_1) \\ u_2 \in T_{\text{D}}(v_2) \end{matrix} \right\}, \quad (5)$$

where T_{D} is the device law of a diode (which is typically monotone), α_R is the reverse short-circuit current ratio and α_F is the forward short-circuit current ratio. These current ratios are usually around 0.9 to 0.995 [14, p. 725]. Figure 3 shows the equivalent circuit representation of this model, as well as a numerical computation of its SRG by sampling random points, which suggests that this operator is angle-bounded. We provide a formal proof of this observation in Proposition IV.4, under the following classical assumption.

Assumption IV.3. T_{NPN} is given by (5), with $\alpha_R, \alpha_F \in [0, 1)$ and $T_{\text{D}} \in \mathcal{M}$ is monotone and outer semicontinuous.

Note that outer semicontinuity of T_{D} ensures by definition that also T_{NPN} is also outer semicontinuous.

Proposition IV.4. *Suppose that Assumption IV.3 holds. Then, T_{NPN} is θ -angle-bounded, where*

$$\theta := \frac{\pi}{2} + \max(\arctan(\alpha_F), \arctan(\alpha_R)).$$

Proof. $T_{\text{NPN}} = R \circ (T_{\text{D}} \times T_{\text{D}})$ is θ -angle-bounded if and only if

$$\angle(x - y, R(u - v)) \leq \theta, \quad \forall (x, u), (y, v) \in \text{gph}(T_{\text{D}} \times T_{\text{D}}).$$

Defining $z := x - y$ and $w := u - v$, this condition holds for any monotone operator T_{D} if and only if

$$\angle(z, R(w)) \leq \theta, \quad \forall z, w \in \mathbb{R}^2 : z_1 w_1 \geq 0, z_2 w_2 \geq 0. \quad (6)$$

If $\|z\| = 0$ or $\|w\| = 0$ then (6) holds vacuously. Otherwise, let $\phi := \text{atan2}(z_2, z_1)$ and $\psi := \text{atan2}(w_2, w_1)$, so that

$$z = \|z\| \begin{bmatrix} \cos(\phi) \\ \sin(\phi) \end{bmatrix} \quad \text{and} \quad w = \|w\| \begin{bmatrix} \cos(\psi) \\ \sin(\psi) \end{bmatrix}.$$

Defining $\delta_k := [-\pi + \frac{\pi}{2}k, -\frac{\pi}{2} + \frac{\pi}{2}k]$, it holds that $z_1 w_1 \geq 0$ and $z_2 w_2 \geq 0$ if and only if there exists a $k \in \{0, 1, 2, 3\}$ such that $\phi, \psi \in \delta_k$. Therefore, by definition of \angle , (6) holds if and only if

$$\arccos \left(\frac{f(\phi, \psi)}{g(\phi, \psi)} \right) \leq \theta, \quad \forall \phi, \psi \in \delta_k, k \in \{0, 1, 2, 3\}, \quad (7)$$

where

$$f(\phi, \psi) := \left\langle \begin{bmatrix} \cos(\phi) \\ \sin(\phi) \end{bmatrix}, R \begin{bmatrix} \cos(\psi) \\ \sin(\psi) \end{bmatrix} \right\rangle,$$

$$g(\phi, \psi) := \|R \begin{bmatrix} \cos(\psi) \\ \sin(\psi) \end{bmatrix}\| > 0,$$

so that

$$\frac{f(\phi, \psi)}{g(\phi, \psi)} = \frac{\cos(\phi - \psi) - \alpha_R \cos(\phi) \sin(\psi) - \alpha_F \sin(\phi) \cos(\psi)}{\sqrt{1 + \alpha_R^2 \sin^2(\psi) - 2(\alpha_R + \alpha_F) \sin(\psi) \cos(\psi) + \alpha_F^2 \cos^2(\psi)}}.$$

If $\phi, \psi \in \delta_1$ or $\phi, \psi \in \delta_3$, then $f(\phi, \psi)$ is lower bounded by zero, and consequently so is $\frac{f(\phi, \psi)}{g(\phi, \psi)}$. If $\phi, \psi \in \delta_0$ or $\phi, \psi \in \delta_2$, then

$$\frac{f(\phi, \psi)}{g(\phi, \psi)} \geq \min \left\{ \frac{-\alpha_F}{\sqrt{1 + \alpha_F^2}}, \frac{-\alpha_R}{\sqrt{1 + \alpha_R^2}} \right\}.$$

Note that this bound is tight and attained for $(\phi, \psi) = (\pi/2, 0)$ if $\alpha_F \geq \alpha_R$ and for $(0, \pi/2)$ otherwise. Therefore, the claim follows directly from (7) by observing that \arccos is a decreasing function and that for any $\alpha \in \mathbb{R}$

$$\arccos \left(\frac{-\alpha}{\sqrt{1 + \alpha^2}} \right) = \frac{\pi}{2} + \arctan(\alpha). \quad \square$$

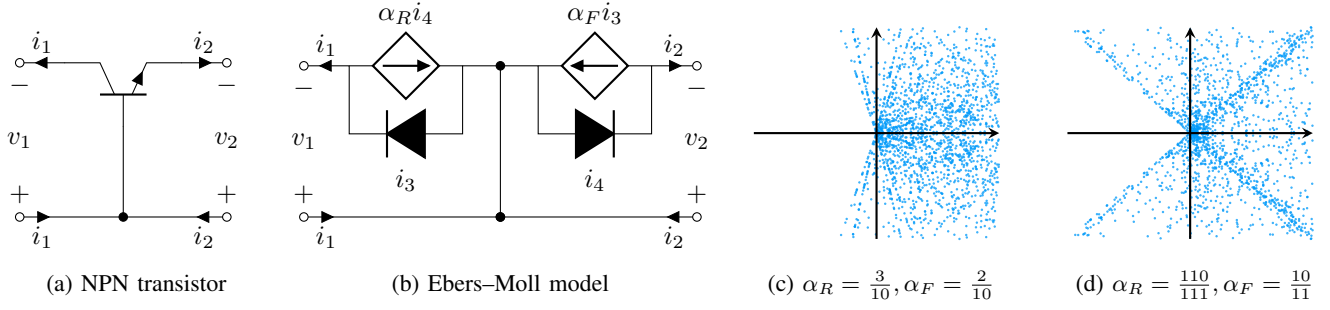


Fig. 3: NPN transistor. (a) Two-port model. (b) Ebers–Moll model. (c)–(d) Numerical SRG of the NPN transistor $G(T_{\text{NPN}})$ for different values of α_R and α_F . In both cases, the incremental angle is upper bounded by 135 degrees.

Corollary IV.5. *Suppose that Assumption IV.3 holds. Then, T_{NPN} is $(\frac{1}{8\rho}, \rho)$ -semimonotone for all $\rho < 0$.*

Proof. By Proposition IV.4, T_{NPN} is $\frac{3\pi}{4}$ -angle-bounded for any $\alpha_F, \alpha_R \in [0, 1)$. The claim then follows immediately from Proposition III.7. \square

V. NONMONOTONE COMMON-EMITTER AMPLIFIERS

In this section, we consider common-emitter amplifiers involving transistors and tunnel diodes, and show that their response can be computed in an efficient manner using Chambolle–Pock.

A. Background on Chambolle–Pock for circuit theory

For many circuits, standard methods of loop and cut-set analysis can be used to find a hybrid representation of the circuit [14]. For instance, denote the internal currents and voltages by respectively $i \in \mathcal{H}^n$ and $v \in \mathcal{H}^m$ and let the influence of the current and voltage sources on the network be given by respectively $s_i \in \mathcal{H}^n$ and $s_v \in \mathcal{H}^m$. Then, the behavior of a circuit can be retrieved by solving an inclusion problem of the form

$$0 \in \begin{bmatrix} R(i) \\ G(v) \end{bmatrix} + \begin{bmatrix} 0 & L^\top \\ -L & 0 \end{bmatrix} \begin{bmatrix} i \\ v \end{bmatrix} + \begin{bmatrix} s_v \\ s_i \end{bmatrix} \quad (8)$$

where $R: \mathcal{H}^n \rightrightarrows \mathcal{H}^n$ and $G: \mathcal{H}^m \rightrightarrows \mathcal{H}^m$ are operators containing respectively the resistive and conductive elements present in the network and the matrix $L \in \mathbb{R}^{m \times n}$ encodes Kirchoff’s current and voltage laws.

A method which is particularly suited for solving inclusion problems of this form is the Chambolle–Pock algorithm (CPA) [8] (also known as the primal-dual hybrid gradient (PDHG) method [15]). When applied to (8), this algorithm performs alternating updates of internal currents and voltages using resolvent computations, where the γ -resolvent of an operator $T: \mathcal{H} \rightrightarrows \mathcal{H}$ is defined as $J_{\gamma T} := (\text{id} + \gamma T)^{-1}$. In particular, for strictly positive stepsizes $\gamma, \tau > 0$, relaxation parameter $\lambda > 0$ and an initial guess $(i^0, v^0) \in \mathcal{H}^n \times \mathcal{H}^m$, CPA is given by

$$\begin{aligned} \bar{i}^k &\in J_{\gamma \bar{R}}(i^k - \gamma L^\top v^k) \\ \bar{v}^k &\in J_{\tau \bar{G}}(v^k + \tau L(2\bar{i}^k - i^k)) \\ i^{k+1} &\in i^k + \lambda(\bar{i}^k - i^k) \\ v^{k+1} &\in v^k + \lambda(\bar{v}^k - v^k) \end{aligned} \quad (\text{CPA})$$

where $\bar{R}(i) := R(i) + s_v$ and $\bar{G}(v) := G(v) + s_i$. The idea of applying CPA for solving (8) was previously explored in [5] in the monotone setting. One of the main advantages of this methodology, besides its scalability, is that it allows R and G to be multi-valued, which standard Newton solvers for electrical circuits are unable to deal with. This advantage also motivates the nonsmooth dynamics framework [16] which is used for simulating analog switched circuits based on complementarity problems and inclusions into normal cones.

B. Implementation details

In all upcoming numerical examples, the transistor parameters are given by $\alpha_R = \frac{110}{111}, \alpha_F = \frac{10}{11}$ and the internal diodes are modeled by ideal diodes, i.e., by

$$T_D: v \mapsto \begin{cases} \{0\}, & \text{if } v < 0, \\ [0, +\infty), & \text{if } v = 0. \end{cases}$$

We denote the transistor voltages by v_1 and v_2 . For numerical simulations, the iterations are stopped once the norm of the relative difference between successive iterates is less than $\epsilon = 10^{-8}$. We do not explicitly verify that the resolvent has full domain, as this assumption mainly ensures the global well-definedness of iterates. No such domain-related issues were encountered in any of our simulations.

C. Examples

First, consider the NPN transistor shown in Figure 4(a), which includes two leakage resistors with resistance $r \gg 1$. For this model, the voltages $v = (v_1, v_2)$ which yield a desired current $i = (i_1, i_2)$ can be obtained by solving the following inclusion problem:

$$\begin{pmatrix} i_1 \\ i_2 \end{pmatrix} \in T_{\text{NPN}} \begin{pmatrix} v_1 \\ v_2 \end{pmatrix} + \frac{1}{r} \begin{pmatrix} v_1 \\ v_2 \end{pmatrix}. \quad (9)$$

As established in Proposition IV.4, an NPN transistor is $\frac{3\pi}{4}$ -angle-bounded under standard assumptions summarized in Assumption IV.3. Therefore, for any $r > 0$ it holds that $T_{\text{NPN}, r} := T_{\text{NPN}} + \frac{1}{r}\text{id}$ is

- (i) $\frac{r(1-\sqrt{2})}{2}$ -comonotone owing to Corollary III.8,
- (ii) $(\frac{1}{2r}, -\frac{r}{2})$ -semimonotone owing to Proposition III.7.

The following proposition demonstrates how this result can be leveraged to solve (9) directly using the proximal point

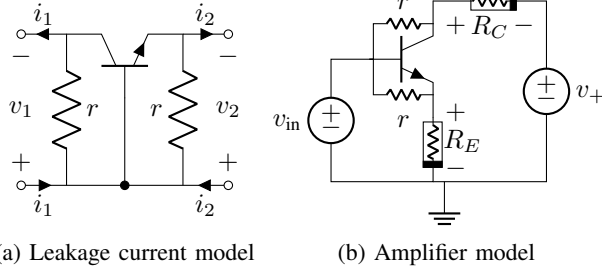


Fig. 4: Common-emitter amplifier with leakage current.

algorithm (PPA), using known convergence results from [10, Thm. 2.4, Tab. 1] in the comonotone setting. This is verified numerically in Figure 5.

Proposition V.1. *Suppose that Assumption IV.3 holds and let $r > 0$. Define $\tilde{T}_{\text{NPN},r}(v) := T_{\text{NPN},r}(v) - i$. Then, any sequence $(v^k)_{k \in \mathbb{N}}$ satisfying the PPA update rule*

$$v^{k+1} \in J_{\gamma \tilde{T}_{\text{NPN},r}}(v^k)$$

with stepsize $\gamma > r(\sqrt{2} - 1)$ converges to a solution of (9).

Proof. Follows directly from [10, Thm. 2.4], since $\tilde{T}_{\text{NPN},r}$ is outer semicontinuous and $\frac{r(1-\sqrt{2})}{2}$ -comonotone. \square

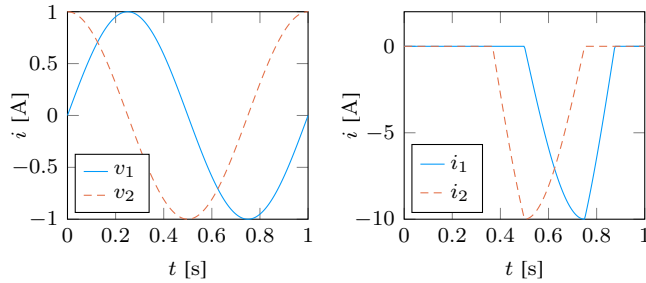


Fig. 5: Solution of inclusion problem (9) with leakage resistance $r = 10 \Omega$ for a given desired sinusoidal current i . The solution has been obtained after 27 proximal point iterations with constant stepsize $\gamma = r > r(\sqrt{2} - 1)$.

In what follows, we connect the nonmonotone element $T_{\text{NPN},r}$ in a so-called common-emitter amplifier circuit, visualized by Figure 4(b). Denote the voltage sources by $v_{\text{in}} \in \mathbb{R}$ and $v_+ \in \mathbb{R}_{++}$. With a suitable convention of the directions of the internal currents and voltages, the response of this network is given by (8), where

$$\begin{aligned} R &:= R_C \times R_E, & G &:= T_{\text{NPN},r}, & L &:= I_2, \\ s_v &:= \begin{pmatrix} v_+ - v_{\text{in}} \\ -v_{\text{in}} \end{pmatrix}, & s_i &:= 0. \end{aligned} \quad (10)$$

By leveraging the convergence results for CPA from [11], we show in the following proposition that the response of this common-emitter amplifier circuit can be computed by CPA under suitable conditions on R_E and R_C and corresponding stepsize conditions. Specifically, Proposition V.2(i) considers the setting where the resistances are strongly monotone,

for which a numerical example is provided in Figure 6, while Proposition V.2(ii) considers the setting where they are merely $(\frac{9}{8}r, -\frac{1}{8r})$ -semimonotone. This latter setting includes resistances which have a *negative resistance region* and is illustrated numerically in Figure 7.

Proposition V.2. *Consider problem (8), where R, G, L, s_v and s_i are defined as in (10). Suppose that Assumption IV.3 holds, that the leakage resistance $r > 0$ and that the (nonlinear) operators $R_C : \mathbb{R} \rightarrow \mathbb{R}$ and $R_E : \mathbb{R} \rightarrow \mathbb{R}$ in (10) are outer semicontinuous. Suppose that R_C and R_E are*

(i) (either) σ -monotone for some $\sigma > \frac{r(\sqrt{2}-1)}{2}$ and

$$\tau \in (\underline{\tau}, +\infty), \gamma \in (0, 1/\tau), \lambda \in (0, 2(1 - \tau/\tau)),$$

$$\text{where } \underline{\tau} := -\frac{\sigma r(1-\sqrt{2})}{r(1-\sqrt{2})+2\sigma},$$

(ii) (or) $(\frac{9}{8}r, -\frac{1}{8r})$ -semimonotone and

$$\gamma \in (\underline{\gamma}, \bar{\gamma}), \tau \in (1/\bar{\gamma}, 1/\gamma), \lambda \in (0, 2(1 - \frac{1}{6r\gamma} - \frac{9}{10r})),$$

$$\text{where } \underline{\gamma} := \frac{5-\sqrt{10}}{9r} \text{ and } \bar{\gamma} := \frac{5+\sqrt{10}}{9r}.$$

Then, any sequence $(i^k, v^k)_{k \in \mathbb{N}}$ generated by (CPA) with stepsizes γ and τ and relaxation parameter λ converges to a solution of (8).

Proof. Note that both \tilde{R} and \tilde{G}^{-1} are outer semicontinuous.

- (i) Follows directly from [11, Cor. 5.4], using that \tilde{R} is σ -monotone and \tilde{G}^{-1} is $\frac{r(1-\sqrt{2})}{2}$ -monotone (since $\tilde{G} = G$ is $\frac{r(1-\sqrt{2})}{2}$ -comonotone).
- (ii) By assumption, \tilde{R} is $(\frac{9}{8}r, -\frac{1}{8r})$ -semimonotone and \tilde{G}^{-1} is $(-\frac{r}{2}, \frac{1}{2r})$ -semimonotone. The claim then follows from [11, Cor. 5.4] with $\beta_P = -\frac{1}{6r}$, $\beta_D = -\frac{9}{10r}$. \square

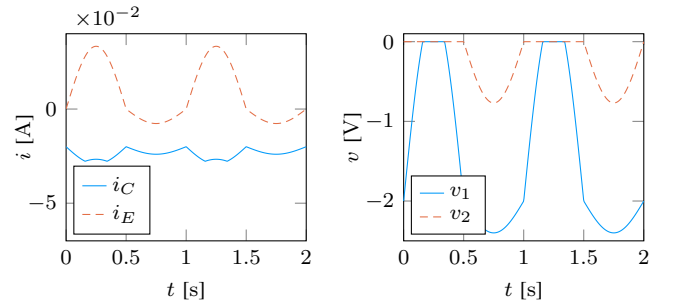


Fig. 6: Calculated internal variables i_C, i_E, v_1, v_2 for the common-emitter amplifier with linear resistors $R_E = r_E \text{id}$ and $R_C = r_C \text{id}$, where $r_E, r_C > \frac{r(\sqrt{2}-1)}{2}$. The circuit parameters are $v_{\text{in}} = \sin(2\pi t) \text{V}$, $v_+ = 5 \text{V}$, $r_E = 30 \Omega$, $r_C = 150 \Omega$ and $r = 100 \Omega$. These internal variables were obtained using Chambolle-Pock after 617 iterations with stepsizes $\gamma = 0.001$, $\tau = 700$ and relaxation parameter $\lambda = 1$.

VI. CONCLUSION

In this work, we derived analytical expressions for the scaled relative graphs of semimonotone and incrementally angle-bounded operators, establishing a connection between the

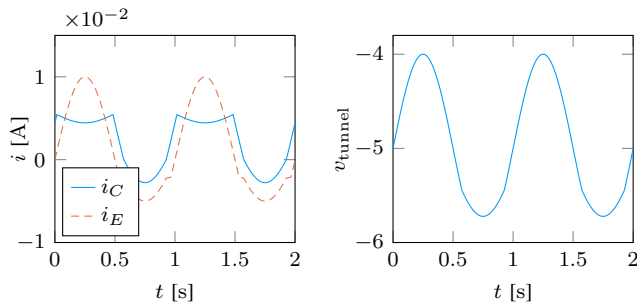


Fig. 7: Calculated internal variables $i_C, i_E, v_{\text{tunnel}}$ for the common-emitter amplifier with a linear resistor $R_E = r_E \text{id}$ and a (multi-valued) resistor $R_C = T_{\text{tunnel}}^{-1}$ defined as the inverse of the tunnel diode in Example IV.2. The circuit parameters are $v_{\text{in}} = \sin(2\pi t) \text{V}$, $v_+ = 5 \text{V}$, $r = 100 \Omega$ and $r_E = 100 \Omega$. The tunnel diode parameters are $r_1 = 100 \Omega$, $r_2 = 900 \Omega$ and $\bar{v} = 5 \text{V}$. Based on Proposition IV.1, it can be shown that R_E and R_C are $(\frac{900}{8}, -\frac{1}{800})$ -semimonotone and the conditions of Proposition V.2(ii) are satisfied. These internal variables were obtained using Chambolle–Pock after 223 iterations with stepsizes $\gamma = \frac{5}{9r} = 1/180$, $\tau = \frac{8r}{5} = 160$ and relaxation parameter $\lambda = 1/4$. Note that both the positive and negative resistance regions of the tunnel diodes are encountered during this experiment.

two classes. We showed that these classes capture the incremental behavior of an Ebers–Moll transistor, enabling us to efficiently compute the response of a nonsmooth and multi-valued common-emitter amplifier circuit with transistors and tunnel diodes using the Chambolle–Pock algorithm.

Future research directions include exploring additional non-monotone elements like nonlinear capacitors, inductors, and memristors, as well as using the SRG to design circuits with specific input-output behavior.

REFERENCES

- [1] E. K. Ryu, R. Hannah, and W. Yin, “Scaled relative graphs: Non-expansive operators via 2D Euclidean geometry,” *Mathematical Programming*, pp. 1–51, 2021.
- [2] T. Chaffey, F. Forni, and R. Sepulchre, “Graphical nonlinear system analysis,” *IEEE Transactions on Automatic Control*, vol. 68, no. 10, pp. 6067–6081, 2023.
- [3] J. Eckstein and D. P. Bertsekas, “On the Douglas–Rachford splitting method and the proximal point algorithm for maximal monotone operators,” *Mathematical Programming*, vol. 55, pp. 293–318, 1992.
- [4] P. Giselsson and S. Boyd, “Linear convergence and metric selection for Douglas–Rachford splitting and ADMM,” 2016. arXiv: 1410.8479.
- [5] T. Chaffey, S. Banert, P. Giselsson, and R. Pates, “Circuit analysis using monotone+skew splitting,” *European Journal of Control*, p. 100854, 2023.
- [6] T. Chaffey and R. Sepulchre, “Monotone one-port circuits,” *IEEE Transactions on Automatic Control*, vol. 69, no. 2, pp. 783–796, 2024.
- [7] B. Tellegen, “A general network theorem, with applications,” *Philips Research Reports*, vol. 7, pp. 259–269, 1952.
- [8] A. Chambolle and T. Pock, “A first-order primal-dual algorithm for convex problems with applications to imaging,” *Journal of Mathematical Imaging and Vision*, vol. 40, no. 1, pp. 120–145, 2011.
- [9] A. L. Hodgkin and A. F. Huxley, “The components of membrane conductance in the giant axon of loligo,” *The Journal of physiology*, vol. 116, no. 4, p. 473, 1952.

- [10] B. Evens, P. Pas, P. Latafat, and P. Patrinos, “Convergence of the preconditioned proximal point method and Douglas–Rachford splitting in the absence of monotonicity,” 2023. arXiv: 2305.03605.
- [11] B. Evens, P. Latafat, and P. Patrinos, “Convergence of the Chambolle–Pock algorithm in the absence of monotonicity,” 2023. arXiv: 2312.06540.
- [12] A.-M. Huijzer, A. van der Schaft, and B. Besselink, “Modelling of memristor networks and the effective memristor,” *Automatica*, vol. 171, p. 111922, 2025.
- [13] C. Chen, W. Chen, D. Zhao, S. Z. Khong, and L. Qiu, “The singular angle of nonlinear systems,” Sept. 2021. arXiv: 2109.01629.
- [14] C. A. Desoer and E. S. Kuh, *Basic circuit theory*. New York: McGraw-Hill, 1969.
- [15] M. Zhu and T. Chan, “An efficient primal-dual hybrid gradient algorithm for total variation image restoration,” *Ucla Cam Report*, vol. 34, pp. 8–34, 2008.
- [16] V. Acary, O. Bonnefon, and B. Brogliato, *Nonsmooth Modeling and Simulation for Switched Circuits*, vol. 69 of *Lecture Notes in Electrical Engineering*. Dordrecht: Springer Netherlands, 2011.